〈일반논문〉
Journal of the Korean Society of Visualization, Vol. 22, No. 2 (35~43), 2024
(Manuscript received : 2024.06.20./Revised : 2024.07.05./Accepted : 2024.07.05.)
DOI:http://dx.doi.org/10.5407/jksv.2024.22.2.035

ISSN 1598-8430 Print
ISSN 2093-808X Online

탄성 및 강성 마이크로입자의 음향미세유체역학적 분리

무스타크 알리* · 이송하* · 박진수†

Acoustofluidic Separation of Elastic and Rigid Microspheres

Mushtaq Ali*, Song Ha Lee*, Jinsoo Park†

Abstract Microparticle separation has demonstrated significant potential for biological, chemical, and medical applications. We introduce a surface acoustic wave (SAW)-based microfluidic device for separation of elastic and rigid microspheres based on their property and size. By tuning the SAWs to match the resonant frequencies of certain microspheres, those particles could be selectively separated from the other microspheres. When microspheres are exposed to an acoustic field, they experience the SAW-induced acoustic radiation force (ARF), whose magnitude is dependent on the microparticle size and properties. We modeled the SAW-induced ARF based on elastic sphere theory and conducted a series of experiments to separate elastic and rigid microspheres. We further utilized the acoustofluidic method for the separation of Thalassiosira Eccentrica microalgae based on the differences in their sizes with purity exceeding 90%. We anticipate that our technique will open up new possibilities for sample preparation, detection, and diagnosis in various emerging biological and medical analyses.

Key Words : Surface Acoustic Wave (표면파), Acoustofluidics (음향미세유체역학), Acoustic Radiation Force (음향방사력), Microparticle (마이크로입자)

1. Introduction

The separation of microspheres is crucial in various biological and medical applications, including drug screening[1], disease diagnosis[2], and cell biology[3]. To achieve high purity, yield, versatility, and biocompatibility in bioparticle separation, researchers are continuously developing new technologies based on different physical principles such as magnetophoresis[4], dielectrophoresis[5], acoustofluidics[6], hydrodynamics[7], and photopheresis[8].

Over the past decade, the use of acoustofluidic using the surface acoustic waves (SAW) for the separations of microspheres in microfluidic channels has shown significant potential due to its ability to separate particles without labeling, its low power consumption, and its high precision and versatility. SAW-based systems can be classified into either traveling wave devices or standing wave devices,

† Department of Mechanical Engineering, Chonnam National University, Republic of Korea
Associate Professor
E-mail: jinsoopark@jnu.ac.kr
* Department of Mechanical Engineering, Chonnam National University, Republic of KoreaGraduate Student

based on the primary mode of wave propagation within the microfluidic channels. A thorough understanding of the formation of complex acoustic fields within the fluidic domain and the resulting manipulation of suspended micro-objects is still demanding. Recently, SAW-based devices have been successfully utilized for various applications, including heating fluids[9], sorting cells[10], manipulating droplets[11], controlling particles[12], nebulizing liquids[13], mixing laminar flows[14], and handling microorganisms[15].

The majority of the available separation techniques are associated with the size of the microspheres. Several studies have explored manipulating microspheres based on their mechanical properties such as density or compressibility rather than their size. Bourquin *et al.*[16] altered the density of the medium relative to suspended RBCs to separate malaria-infected cells from healthy cells within a sessile droplet. Augustsson *et al.*[17] utilized bulk acoustic waves to focus cells regardless of size by adjusting fluid density gradients in a microchannel. Destgeer *et al.*[18] demonstrated separating elastic polystyrene and poly (methyl methacrylate) particles of similar size but different material properties. Ma *et al.*[19] also utilized differences in mechanical properties to effectively separate PS and PMMA particles of similar sizes by adjusting the frequency of applied SAWs. The nonlinear responses of particles to SAWs, influenced by their resonant frequencies, enabled size-independent manipulation. However, the experimental validation of manipulating larger particles with elastic properties remains relatively unexplored in these studies. It is worth noting that there exist certain biological cells, such as microalgae, cancer cells, and a few mammalian cells, that fall within the size range of a few tens of micrometers.

In this research, we proposed an acoustofluidic device capable of manipulating elastic and rigid microspheres. The elastic and rigid microspheres responded differently to the SAW amplitudes based on their individual resonant frequencies. By tuning the SAWs to match the resonant frequencies of certain microspheres, those particles could be selectively manipulated and separated from the other microspheres. We conducted and analyzed experiments with varying acoustic power while maintaining consistent flow conditions to keep the flow-induced drag force constant. A cross-type microfluidic chip is used, consisting of a slanted finger interdigital transducer (SFIT) on a piezoelectric substrate, so that SAW is applied perpendicular to the flow direction. SAW-induced ARF was analyzed using elastic sphere theory. Based on the experimental findings of the microspheres, we implemented our technique to separate microalgae of varying sizes.

2. Methodology

Fig. 1 depicts the schematic diagram of the cross-type microfluidic device utilized in this study. The device includes a slanted finger interdigital transducer (SFIT) made of a bilayer of metallic materials (Cr and Au) deposited on a piezoelectric lithium niobate (LN) substrate (128° Y-X cut, 0.5-mm thick, 4-inch diameter, MTI Korea). A polydimethylsiloxane (PDMS) microchannel

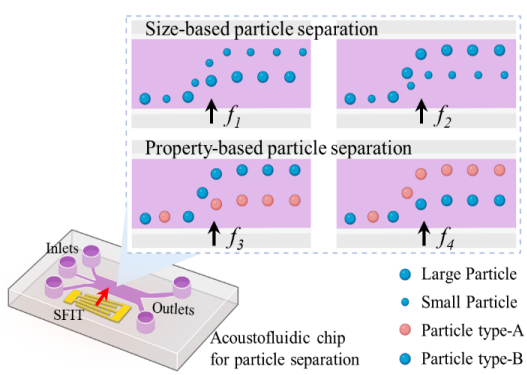

Fig. 1. Schematic diagram of the proposed acoustofluidic device for of elastic and rigid microspheres. The figure was created with BioRender.com.

was bonded to the LN substrate next to the SFIT, ensuring that the acoustic waves generated by the transducer are perpendicular to the direction of fluid flow. The SFIT with finger spacings ($\lambda/4$) of 18.5-24 μm and corresponding to frequency ranges of 41-54 MHz were utilized. The SFIT consists of 30 pairs of fingers with a total aperture of 1500 μm. The resonant frequencies of 46 MHz (first peak) and 51.8 MHz (second peak) were utilized for 15 μm and 20 μm polystyrene (PS) microspheres. The fused silica (FS) microsphere did not exhibit any resonant peak, so they were considered as non-target microspheres for the separation. The PDMS microchannel, fabricated using the soft lithography technique, was securely bonded to the LN substrate using oxygen plasma bonding (Covance, Femto Science). The microchannel has a height of 50 μm, and the width of the main acoustic actuation region is 500 μm. The PDMS microchannel includes three inlets and two outlets. Inlets 1 and 3 were used to introduce sheath fluids (DI water), while inlet 2 was used for injecting the sample fluid containing microspheres. The sheath fluids hydrodynamically focused the suspended microspheres near the bottom microchannel wall. Additionally, the sheath fluids served to prevent the formation of the microchannel anechoic corner, a region with a weak acoustic field that forms in the channel corner due to the oblique propagation of leaky SAW at the Rayleigh angle. Fluids were introduced into the microchannels using a high-precision multi-syringe pump (neMESYS Cetoni GmbH). The microspheres were initially dispersed in DI water solution with 5 wt% TWEEN® 20 to ensure a stable suspension and to avoid the particle clogging within the microchannel.

The Thalassiosira Eccentrica (TE) (LIMS-PS-1759) diatom was obtained from the Korea Institute of Ocean Science & Technology (KIOST). TE is a marine centric diatom characterized by its cylindrical shape, with a diameter of ~11 μm and a height of ~27 μm[20]. Before conducting the experiments, the TE were cultured in 50 mL conical flasks containing saltwater F/2 culture media. They were maintained at room temperature under continuous illumination at an intensity of 3000 lux and shaken at 150 rpm. To prepare the microalgae for the experiments, a 1 mL sample of the cultured algae was placed in a microcentrifuge tube (Hyundai Micro) and centrifuged at 1500 rpm for 5 minutes using a mini centrifuge (Daihan Scientific). Following centrifugation, the microalgae were mixed in fresh growth media and diluted to get a desired cell concentration for further experiments.

When an AC voltage was applied across the terminals of the SFIT, it generated acoustic waves on the LN substrate. These Rayleigh-type SAWs propagated on the substrate and then transmitted into the fluid medium in the form of longitudinal waves[21]. When a solid microsphere suspended in the liquid interacted with the acoustic waves, the acoustic radiation force (ARF) is generated. When acoustic waves enter the fluid medium and interact with the microspheres, it causes inhomogeneous wave scattering at the solid-liquid interface due to differences in acoustic impedance. At the interface between the object and the acoustic medium, partial reflection and transmission of the acoustic wave can occur, contributing to the origination of the ARF. The radiation force induced by traveling acoustic waves is influenced by the anisotropic wave scattering. The ARF arising from the scattering of the primary wave depends significantly on resonant points at specific acoustic frequencies due to the free vibration. The magnitude of ARF in regimes such as Mie, Rayleigh, and geometrical scattering varies depending on factors such as acoustic wave frequency, material properties of the microspheres, and object shape. The ARF on the microparticle in Mie scattering regime can be calculated using the dimensionless parameter called as, ARF factor (ARFF). This dimensionless

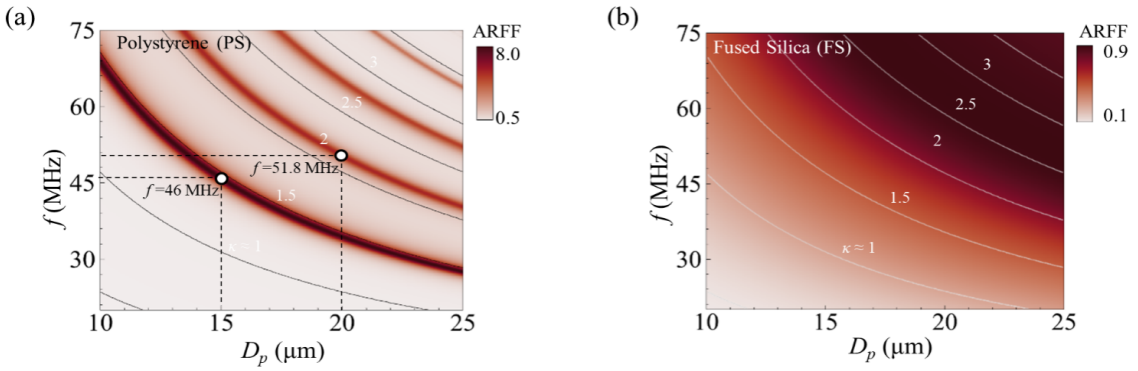

Fig. 2. Contour plot showing the acoustic radiation force factor (ARFF) with varying acoustic wave frequency (f) and a diameter (D_p) for (a) polystyrene (PS) microsphere and (b) fused silica (FS) microspheres

parameter quantifies the force applied to a microparticle per unit acoustic energy density and per unit cross-sectional area of the particle. For elastic particles exposed to traveling SAW, the ARFF is derived using elastic theory of Hasegawa and Yosioka[22]:

$$\mathrm{ARFF} = \langle \mathrm{ARF} \rangle / (\pi {D_p}^2 \bar{E}/4) \tag{1}$$

where, D_p, and $\bar{E}$ represent the time-averaged acoustic radiation force, microsphere diameter, and mean energy density, respectively.

$$\langle \mathrm{ARF} \rangle = -\frac{4}{k^2}\sum_{n=0}^{\infty}[(P_n+1)(P_n+P+2P_nP_{n+1}+2Q_nQ_{n+1})] \tag{2}$$

$$P_n = -\frac{[F_n j_n(\kappa) - \kappa j_n'(\kappa)]^2}{[F_n j_n(\kappa) - \kappa j_n'(\kappa)]^2 + [F_n n_n(\kappa) - \kappa n_n'(\kappa)]^2} \tag{3}$$

$$Q_n = -\frac{[F_n j_n(\kappa) - \kappa j_n'(\kappa)][F_n n_n(\kappa) - \kappa n_n'(\kappa)]}{[F_n j_n(\kappa) - \kappa j_n'(\kappa)]^2 + [F_n n_n(\kappa) - \kappa n_n'(\kappa)]^2} \tag{4}$$

$$F_n = \frac{\kappa_2^2 \rho_f}{2\rho_p} \cdot \frac{\frac{\kappa_1 j_n'(\kappa_1)}{\kappa_1 j_n'(\kappa_1) - j_n(\kappa_1)} - \frac{2n(n+1) j_n(\kappa_2)}{(n+2)(n-1) j_n(\kappa_2) + \kappa_2^2 j_n''(\kappa_2)}}{\frac{\sigma}{\kappa_1^2[1-2\sigma j_n(\kappa_1)} - j_n'(\kappa_1)]} - \frac{2n(n+1)[j_n(\kappa_2) - \kappa_2 j_n'(\kappa_2)}{(n+2)(n-1) j_n(\kappa_2) + \kappa_2^2 j_n''(\kappa_2)} \tag{5}$$

where, j_n, F_n, ρ_f, ρ_p, σ are represent the spherical Bessel function of the order n, scattering coefficient of the incident wave, density of the fluid, particle density and the Poisson ratio, respectively.

To characterize the motion of microspheres with a diameter D_p suspended in a fluid when exposed to acoustic waves with frequency wavelength λ_f, the Helmholtz number $x = \pi D_p/\lambda_f$ is an important parameter. As the insets in Fig. 1 reflect that based on the resonant frequencies of the individual, the size–based as well as property–based separation can be achieved. The ARF magnitude and thus deflection of an individual particle from a group of particles with different sizes (PS 15 μm and PS 20 μm) or different material properties (15 μm PS and FS, and 20 μm PS and FS) varies due to their non-linear responses to the acoustic waves when $x > 1$. Fig. 2(a) shows the ARFF factor plot for PS microsphere as a function of the particle diameter D_p. The figure illustrates that the ARF factor exhibits a specific relationship between the $f - D_p$ relationship where there is a one-to-one correlation observed between f and D_p for efficient particle separation based on the SAW-induced ARF. Fig. 2(b) shows the ARF factor plot for FS microspheres. It can be observed

that compared to PS microspheres, FS microspheres do not possess distinct resonance frequencies corresponding to the size of the particles. The resonant peaks relate to subsequent modes of particle vibration and are significant in the PS graphs but not in that of FS. This behavior is expected because the FS microspheres are more rigid than the elastic PS microspheres as the elastic modulus values of PS and FS are ~3400 MPa[23] and ~73,000 MPa[24], respectively.

3. Results and Discussion

By leveraging the resonant peaks and the dependence of the ARF on the elastic properties of the particles, it becomes possible to selectively manipulate and separate particles based on their size as well as material characteristics. Firstly, a mixture of PS microspheres having diameters of 15 and 20 μm was pumped through the microchannel and exposed to SAWs. The fluid in which particles were suspended into the microchannel at an inlet flow rate of 100 μL/h, while two sheath fluids from above and below inlets were introduced at a flow rate of 200 and 1500 μL/h. The sheath flow rates were adjusted in such a way that particles aligned near to the microchannel walls and to avoid microchannel anechoic corner effect. The sheath fluids also serve to control the speed of the particles. With this setup, these particles can now experience the SAWs, and their deflections can be observed. The first effective frequency of PS 15 μm was noted to be 46 MHz on the basis of our theoretical estimation in Fig. 2(a). The stacked experimental microscopic images in Fig. 3 (a) shows a particle separation when the PS 15 μm was chosen as a target microsphere. It can be seen in the figure that PS 15 μm microspheres were deflected more as compared to PS 20 μm microspheres at f = 46 MHz, ultimately achieving separation. The phenomenon can be attributed to

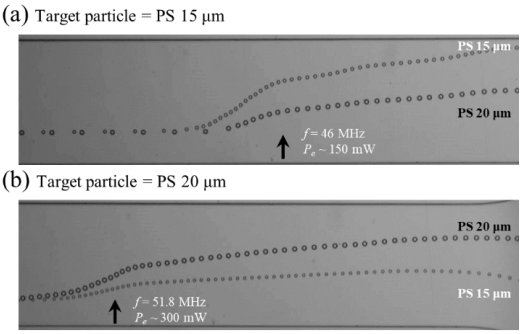

Fig. 3. (a) Stacked microcopy images of particles based on size when target particle was PS 15 μm. (a) Stacked microcopy images of particles based on size when target particle was PS 20 μm

the elastic properties of the PS microspheres. When the SAW frequency matches the resonant frequency of a specific particle size, the particles experience enhanced vibrations, leading to stronger scattering of the acoustic wave. This resonant behavior results in an amplification of the ARF acting on those particles, causing them to deflect more compared to particles of different sizes. In these experiments, an acoustic power (Pe) of 150 mW was utilized. The acoustic power level was carefully selected to achieve two key objectives first, to ensure the particles underwent substantial lateral migration, and second, to facilitate clear separation between the two particle types. It is also important to note that excessive acoustic power can force particles too close to the microchannel wall, which negatively impacts separation efficiency. To avoid this, the acoustic power was fine-tuned to maintain particle positioning away from the channel walls. The input power was adjusted accordingly to meet these experimental requirements. In the another set of experiments, PS 20 μm was selected as a target particle and the effective frequency of 51.8 MHz was chosen. It is to be noted that the chosen frequency is the second effective frequency for the PS 20 μm particles, which was selected based on the availability of the

SFIT. These experimental results suggest that by carefully selecting the appropriate effective frequency for the target particle size, the ARF can be optimized to achieve the desired separation.

Furthermore, the study was extended to separate microspheres based on their material properties. PS and FS microspheres have distinct material properties; specifically, the elastic modulus of PS is lower than that of FS. Consequently, PS can be classified as an elastic microsphere, whereas FS is considered a rigid microsphere. As explained earlier, for elastic microspheres such as PS, when the SAW frequency matches the resonant frequency of a specific particle size, the particles experience enhanced vibrations, leading to stronger scattering of the acoustic wave. This resonant behavior results in an amplification of the ARF acting on those particles, causing them to deflect more compared to particles of different sizes or material properties. This mechanism was applied to separate PS microspheres from FS microspheres. By tuning the SAW frequency to match the resonant frequencies, the PS microspheres experience amplified ARF, resulting in significant deflection and enabling separation. In contrast, FS microspheres, being rigid, do not possess the same resonant behavior as elastic microspheres. As a result, they do not exhibit distinct resonant peaks corresponding to their size, and their deflection is expected to be less compared to the PS microspheres at the same acoustic frequencies. Fig. 4(a) shows the separation of equal sized microspheres based on the material properties

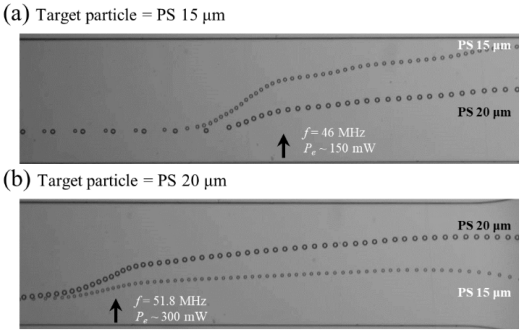

Fig. 3. (a) Stacked microcopy images of particles based on size when target particle was PS 15 μm. (a) Stacked microcopy images of particles based on size when target particle was PS 20 μm

when the target particles were chosen as PS 15 μm. When the resonant frequency of 46 MHz was applied, the PS microspheres were deflected more as compared to the FS microspheres. The phenomenon is attributed to the elastic behavior of the PS microsphere. Similar phenomena was observed in the Fig. 4(b) while separating 20 μm (FS and PS). When the second resonant peak of PS 20 μm of 51.8 MHz was utilized, the PS microspheres experienced a greater magnitude of ARF because of subsequent modes of particle vibration. On the other hand, FS particles do not possess any resonance mode of free vibration.

4. Separation of microalgae

To demonstrate the applicability of our proposed device, we conducted a separation of microalgae based on their size. TE is cylindrical microalgae with a polydisperse size distribution. Due to the large size distribution of TE microalgae, subsequent

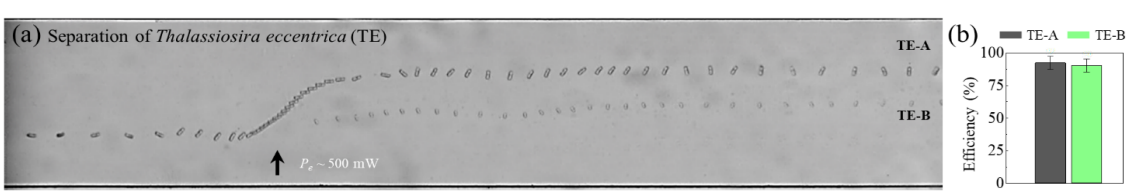

Fig. 5. (a) Stacked microscopy images of size–based separation of Thalassiosira Eccentrica (TE) microalgae. (b) The efficiencies of TE separation in terms of purity.

separation is crucial for certain applications. We utilized our approach to separate two different sized TE microalgae (TE-A and TE-B), as shown in Fig. 5(a). Since TE-A is larger, it experiences a greater magnitude of ARF compared to the smaller TE-B, ultimately achieving separation. The separation efficiencies in terms of purity are shown in Fig. 5(b), with 93.7% for TE-A and 90.1% for TE-B. Hence, the suggested device can effectively screen and isolate particular cells or biosamples, demonstrating the diverse applications of acoustofluidic techniques across multiple fields.

5. Conclusion

This study introduces a SAW-based microfluidic device for the label-free separation of elastic and rigid microspheres based on their properties and sizes. By tuning the SAWs to match the resonant frequencies of specific microspheres, these particles can be selectively separated from others. The proposed device consists of a SFIT on a piezoelectric substrate, with a PDMS microchannel positioned on the substrate. The microchannel is designed in a cross-type layout, allowing the SAWs to propagate perpendicularly to the flow within the channel. When microspheres are exposed to an acoustic field, they experience the SAW-induced ARF, the magnitude of which depends on the size and properties of the microspheres. We modeled the SAW-induced ARF based on elastic sphere theory and conducted a series of experiments to separate elastic and rigid microspheres. Additionally, we applied the acoustofluidic method to separate Thalassiosira eccentrica (TE) microalgae based on size differences, achieving a purity exceeding 90%. We expect that our device will open up new opportunities for sample preparation and diagnosis in various biological and medical analyses.

Acknowledgements

This work was supported by the Korea Industrial Complex Corporation (KICOX) Competitiveness reinforcement project for industrial clusters grants funded by the Korea government (MOTIE) (No. 1415189052). The microfluidic devices were fabricated by using a mask aligner (MDA-400S, MIDAS) at Energy Convergence Core Facility in Chonnam National University.

REFERENCES

1) Fraser, Andrew G., Ravi S. Kamath, Peder Zipperlen, Maruxa Martinez-Campos, Marc Sohrmann, and Julie Ahringer. "Functional genomic analysis of C. elegans chromosome I by systematic RNA interference." Nature 408, no. 6810 (2000): 325-330.
2) Wang, Zeyu, Haichen Wang, Ryan Becker, Joseph Rufo, Shujie Yang, Brian E. Mace, Mengxi Wu, Jun Zou, Daniel T. Laskowitz, and Tony Jun Huang. "Acoustofluidic separation enables early diagnosis of traumatic brain injury based on circulating exosomes." Microsystems & Nanoengineering 7, no. 1 (2021): 20.
3) Xie, Yuliang, Hunter Bachman, and Tony Jun Huang. "Acoustofluidic methods in cell analysis." TrAC Trends in Analytical Chemistry 117 (2019): 280-290.
4) Hejazian, Majid, Weihua Li, and Nam-Trung Nguyen. "Lab on a chip for continuous-flow magnetic cell separation." Lab on a Chip 15, no. 4 (2015): 959-970.
5) Akagi, Takanori, and Takanori Ichiki. "Cell electrophoresis on a chip: what can we know from the changes in electrophoretic mobility?." Analytical and bioanalytical chemistry 391 (2008): 2433-2441.
6) Julio, Raihan Hadi, Muhammad Soban Khan, Mushtaq Ali, Ghulam Destgeer, and Jinsoo

Park. "Size-based Separation of Yeast Cell by Surface Acoustic Wave-induced Acoustic Radiation Force." Journal of the Korean Society of Visualization 21, no. 3 (2023): 93-100.

7) Huang, Lotien Richard, Edward C. Cox, Robert H. Austin, and James C. Sturm. "Continuous particle separation through deterministic lateral displacement." Science 304, no. 5673 (2004): 987-990.

8) MacDonald, Michael P., Gabriel C. Spalding, and Kishan Dholakia. "Microfluidic sorting in an optical lattice." Nature 426, no. 6965 (2003): 421-424.

9) Ha, Byung Hang, Kang Soo Lee, Ghulam Destgeer, Jinsoo Park, Jin Seung Choung, Jin Ho Jung, Jennifer Hyunjong Shin, and Hyung Jin Sung. "Acoustothermal heating of polydimethylsiloxane microfluidic system." Scientific reports 5, no. 1 (2015): 11851.

10) Bhagat, Ali Asgar S., Hansen Bow, Han Wei Hou, Swee Jin Tan, Jongyoon Han, and Chwee Teck Lim. "Microfluidics for cell separation." Medical & biological engineering & computing 48 (2010): 999-1014.

11) Ali, Mushtaq, and Jinsoo Park. "Ultrasonic surface acoustic wave-assisted separation of microscale droplets with varying acoustic impedance." Ultrasonics Sonochemistry 93 (2023): 106305.

12) Destgeer, Ghulam, Byung Hang Ha, Jinsoo Park, Jin Ho Jung, Anas Alazzam, and Hyung Jin Sung. "Travelling surface acoustic waves microfluidics." Physics Procedia 70 (2015): 34-37.

13) Amstad, Esther, Frans Spaepen, Michael P. Brenner, and David A. Weitz. "The microfluidic nebulator: production of sub-micrometer sized airborne drops." Lab on a Chip 17, no. 8 (2017): 1475-1480.

14) Ahmed, Husnain, Jinsoo Park, Ghulam Destgeer, Muhammad Afzal, and Hyung Jin Sung. "Surface acoustic wave-based micromixing enhancement using a single interdigital transducer." Applied Physics Letters 114, no. 4 (2019).

15) Khan, Muhammad Soban, Mushtaq Ali, Song Ha Lee, Keun Young Jang, Seong Jae Lee, and Jinsoo Park. "Acoustofluidic separation of prolate and spherical micro-objects." Microsystems & Nanoengineering 10, no. 1 (2024): 6.

16) Bourquin, Yannyk, Abeer Syed, Julien Reboud, Lisa C. Ranford-Cartwright, Michael P. Barrett, and Jonathan M. Cooper. "Rare-cell enrichment by a rapid, label-free, ultrasonic isopycnic technique for medical diagnostics." Angewandte Chemie International Edition 53, no. 22 (2014): 5587-5590.

17) Augustsson, Per, Jonas T. Karlsen, Hao-Wei Su, Henrik Bruus, and Joel Voldman. "Iso-acoustic focusing of cells for size-insensitive acousto-mechanical phenotyping." Nature communications 7, no. 1 (2016): 11556.

18) Destgeer, Ghulam, Jin Ho Jung, Jinsoo Park, Husnain Ahmed, Kwangseok Park, Raheel Ahmad, and Hyung Jin Sung. "Acoustic impedance-based manipulation of elastic microspheres using travelling surface acoustic waves." RSC advances 7, no. 36 (2017): 22524-22530.

19) Ma, Zhichao, David J. Collins, Jinhong Guo, and Ye Ai. "Mechanical properties based particle separation via traveling surface acoustic wave." Analytical chemistry 88, no. 23 (2016): 11844-11851.

20) Ali, Mushtaq, Song Ha Lee, Beomseok Cha, Woohyuk Kim, Nomin-Erdene Oyunbaatar, Dong-Weon Lee, and Jinsoo Park. "Acoustofluidic separation of cell-encapsulated droplets based on traveling surface acoustic wave-induced acoustic radiation force." Sensors and Actuators B: Chemical (2024): 135988.

21) Sahin, Mehmet A., Mushtaq Ali, Jinsoo Park, and Ghulam Destgeer. "Fundamentals of Acoustic Wave Generation and Propagation." Acoustic Technologies in Biology and Medicine (2023): 1-36.

22) Hasegawa, Takahi, and Katuya Yosioka. "Acoustic-radiation force on a solid elastic sphere." The Journal of the Acoustical Society of America 46, no. 5B (1969): 1139-1143.
23) Brandrup, J., Immergut, E.H., Grulke, E.A., Abe, A. and Bloch, D.R. eds., 1999. Polymer handbook (Vol. 89, pp. V87-V90). New York: Wiley.
24) Hopkins, C.C., Haward, S.J. and Shen, A.Q., 2020. Purely elastic fluid–structure interactions in microfluidics: implications for mucociliary flows. Small, 16(9), p.1903872.